

# A new measurement of the Pontecorvo reaction $\bar{p} + d \rightarrow \pi^- + p$ with the OBELIX spectrometer at LEAR

OBELIX Collaboration

V.G. Ableev <sup>h</sup>, A. Adamo <sup>a</sup>, M. Agnello <sup>b</sup>, F. Balestra <sup>g</sup>, G. Bendiscioli <sup>d</sup>,  
A. Bertin <sup>e</sup>, P. Boccaccio <sup>f</sup>, G. Bonazzola <sup>g</sup>, T. Bressani <sup>g</sup>, M. Bruschi <sup>e</sup>,  
M.P. Bussa <sup>g</sup>, L. Busso <sup>g</sup>, D. Calvo <sup>g</sup>, M. Capponi <sup>c</sup>, P. Cerello <sup>g</sup>, C. Cicalò <sup>a</sup>,  
M. Corradini <sup>c</sup>, S. Costa <sup>g</sup>, S. De Castro <sup>e</sup>, F. D'Isep <sup>g</sup>, A. Donzella <sup>c</sup>,  
I.V. Falomkin <sup>h</sup>, L. Fava <sup>g</sup>, A. Feliciello <sup>g</sup>, L. Ferrero <sup>g</sup>, A. Filippi <sup>g</sup>, V. Filippini <sup>d</sup>,  
D. Galli <sup>e</sup>, R. Garfagnini <sup>g</sup>, U. Gastaldi <sup>f</sup>, P. Gianotti <sup>i</sup>, A. Grasso <sup>g</sup>, C. Guaraldo <sup>i</sup>,  
F. Iazzi <sup>b</sup>, A. Lanaro <sup>i</sup>, E. Lodi Rizzini <sup>c</sup>, M. Lombardi <sup>f</sup>, V. Lucherini <sup>i</sup>,  
A. Maggiora <sup>g</sup>, G. Maneva <sup>h</sup>, S. Marcello <sup>g</sup>, U. Marconi <sup>c</sup>, G.V. Margagliotti <sup>j</sup>,  
G. Maron <sup>f</sup>, A. Masoni <sup>a</sup>, I. Massa <sup>e</sup>, B. Minetti <sup>b</sup>, P. Montagna <sup>d</sup>, M. Morando <sup>k</sup>,  
F. Nichitiu <sup>i</sup>, D. Panziera <sup>g</sup>, G. Pauli <sup>j</sup>, M. Piccinini <sup>e</sup>, G. Piragino <sup>g</sup>, M. Poli <sup>l</sup>,  
G.B. Pontecorvo <sup>h</sup>, G. Puddu <sup>a</sup>, R.A. Ricci <sup>f,k</sup>, E. Rossetto <sup>g</sup>, A. Rotondi <sup>d</sup>,  
A.M. Rozhdestvensky <sup>h</sup>, P. Salvini <sup>d</sup>, L. Santi <sup>m</sup>, M.G. Sapozhnikov <sup>h</sup>,  
N. Semprini Cesari <sup>c</sup>, S. Serci <sup>a</sup>, R. Spighi <sup>e</sup>, P. Temnikov <sup>a</sup>, S. Tessaro <sup>j</sup>,  
F. Tosello <sup>g</sup>, V.I. Tretyak <sup>d</sup>, G. Usai <sup>a</sup>, L. Vannucci <sup>f</sup>, S. Vecchi <sup>e</sup>, G. Vedovato <sup>f</sup>,  
L. Venturelli <sup>c</sup>, M. Villa <sup>e</sup>, A. Vitale <sup>e</sup>, A. Zenoni <sup>n</sup>, A. Zoccoli <sup>e</sup>, G. Zosi <sup>g</sup>

<sup>a</sup> Dip. di Scienze Fisiche, Università di Cagliari and INFN Sez. di Cagliari, I-09100 Cagliari, Italy

<sup>b</sup> Politecnico di Torino and INFN Sez. di Torino, I-10125 Torino, Italy

<sup>c</sup> Dip. di Elettronica per l'Autom. Industriale, Università di Brescia and INFN Sez. di Torino, I-25060 Brescia, Italy

<sup>d</sup> Dip. di Fisica Nucl. e Teor., Università di Pavia and INFN Sez. di Pavia, I-27100 Pavia, Italy

<sup>e</sup> Dip. di Fisica, Università di Bologna and INFN Sez. di Bologna, I-40100 Bologna, Italy

<sup>f</sup> Laboratori Nazionali di Legnaro dell' INFN, I-35100 Padova, Italy

<sup>g</sup> Istituto di Fisica, Università di Torino and INFN Sez. di Torino, I-10125 Torino, Italy

<sup>h</sup> Joint Institute for Nuclear Research, Dubna, SU-101000 Moscow, Russia

<sup>i</sup> Laboratori Nazionali di Frascati dell' INFN, I-00044 Frascati, Italy

<sup>j</sup> Istituto di Fisica, Università di Trieste and INFN Sez. di Trieste, I-34127 Trieste, Italy

<sup>k</sup> Dip. di Fisica, Università di Padova and INFN Sez. di Padova, I-35100 Padova, Italy

<sup>l</sup> Dip. di Energetica, Università di Firenze and INFN Sez. di Bologna, I-40100 Bologna, Italy

<sup>m</sup> Istituto di Fisica, Università di Udine and INFN Sez. di Trieste, I-33100 Udine, Italy

<sup>n</sup> Dip. di Elettronica per l'Autom. Industriale, Università di Brescia and INFN Sez. di Pavia, I-27100 Pavia, Italy

Received 19 February 1993

**Abstract**

Antinucleon–nucleus annihilations into two-body final states containing only one or no meson are unusual annihilations (Pontecorvo reactions), practically unexplored experimentally, with the exception of the channel  $\bar{p}d \rightarrow \pi^- p$ , for which only two low-statistics measurements exist. Their physical interest lies in the possibility of exploring small-distance nuclear dynamics, in which an important role can be played by non-nucleonic degrees of freedom. A new measurement of the  $\bar{p}d \rightarrow \pi^- p$  reaction rate at rest, performed with the OBELIX spectrometer at LEAR, with the best statistics up to now and a careful evaluation of systematic effects is reported, together with a critical analysis of the existing theoretical models. The measured branching ratio, which confirms the previous results, can represent a reference point for the studies in the field.

*Key words:* NUCLEAR REACTIONS  $d(\bar{p}, p\pi^-)$ ,  $E$  at rest; measured absolute branching ratio. OBELIX spectrometer.

**1. Introduction**

The so-called Pontecorvo reactions [1] constitute a wide class of antinucleon annihilation reactions on nuclei, characterized by two-body final states consisting of a *baryon–meson* or a *baryon–baryon* pair.

The simplest Pontecorvo reactions are the:

*Single-meson annihilations*, in which the meson is a *pion*, for example:

$$\bar{p} + d \rightarrow \pi^- + p, \quad (1.1)$$

$$\bar{p} + d \rightarrow \pi^0 + n, \quad (1.2)$$

or a *meson resonance*:

$$\bar{p} + d \rightarrow M + N, \quad (1.3)$$

where M stands for  $\eta, \rho, \omega \dots$ , and N is a nucleon.

In an ordinary  $\bar{N}N$  annihilation at least two mesons must be produced. The process where an antinucleon–nucleon pair is converted into a single meson is forbidden on free nucleons, because the conservation of momentum and energy cannot be satisfied simultaneously. For that reason, the processes (1.1)–(1.3), the Pontecorvo reactions, in which only one meson is the product of the annihilation, are called *unusual annihilations*.

As for other processes in nuclear physics, energy–momentum conservation in Pontecorvo reactions can be satisfied by allowing the process to proceed via the contribution of at least two nucleons. A “multinucleon” annihilation presents indeed strong reasons of interest: small-distance dynamics between nucleons of nuclei, where quark degrees of freedom play an important role, must determine the amplitude of reactions.

Despite the motivations, Pontecorvo reactions have not yet been experimentally measured, with the only exception of the reaction (1.1) at rest, for which two only published results exist, both statistically poor.

They rely upon 6 bubble chamber events [2], providing a branching ratio:

$$\text{BR}(\bar{p} d \rightarrow \pi^- p) = N(\bar{p} d \rightarrow \pi^- p) / N(\bar{p} d \rightarrow \text{all}) = 0.9 \pm 0.4 \times 10^{-5} \quad (1.4)$$

and on 5 events measured by the ASTERIX Collaboration at LEAR [3], yielding a branching ratio:

$$\text{BR}(\bar{p} d \rightarrow \pi^- p) = 1.4 \pm 0.7 \times 10^{-5}. \quad (1.5)$$

A new measurement of antiproton absorption in deuterium gas, with the best statistics up to now and a careful evaluation of systematic effects was performed using the OBELIX spectrometer at LEAR. The result confirms the previous measurements and can represent a reference point in the investigation of Pontecorvo reactions.

The paper is organized as follows. Sect. 2 contains a critical review of the existing theoretical descriptions of Pontecorvo reactions, aimed to clarify their physical meaning. In sect. 3, the experimental technique followed in the OBELIX measurement is described in detail. In sect. 4, data analysis procedures are discussed and the result of the measurement is reported. Sect. 5 contains the concluding remarks together with a look to some perspectives in the field.

## 2. The physics of Pontecorvo reactions

The study of Pontecorvo reactions has proceeded along the following lines:

- (i) Consideration of two-step hadron–nucleus sub-processes;
- (ii) Regge-pole approach, taking advantage of the principle of crossing symmetry;
- (iii) Statistical model, applied to the decay of a fireball with baryonic number  $b > 0$ .

### 2.1. Two-step hadron–nucleus sub-processes

The simplest way to describe the “prototype” Pontecorvo reaction



is to consider a two-step process described by the triangle diagram of fig. 1. In the first step, two mesons are produced after an elementary annihilation:



and then it is assumed [4–7] that one of the produced mesons is absorbed by the spectator nucleon. Since the created mesons are highly energetic ( $T_{\text{kin}} \approx m_N$ ), if

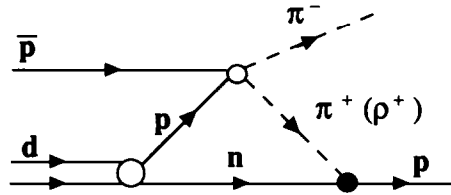


Fig. 1. Diagram describing the two-step mechanism in the reaction  $\bar{p} d \rightarrow \pi^- p$ .

nucleons of deuteron are close to their mass-shell, the process of absorption cannot conserve energy-momentum at each step and the exchanged meson is very far off mass-shell. For annihilation at rest, for example, the invariant variable  $t = -q^2$ , where  $q$  is the four-momentum transfer, which gives the mass of the “meson” in the intermediate state (and then its degree of virtuality), turns out to be

$$t \approx -1.2 \text{ GeV}^2. \quad (2.3)$$

Therefore, estimates of the cross section of reaction (2.1) strongly depend on the behaviour of both the virtual meson form factor, and the deuteron wave function at small distance (or, accordingly, its high-momentum components). The dependence on virtuality  $q^2$  has been parametrized by form factors of monopole and dipole type [4]:

$$F(q^2) = \frac{(\mu^2 - \Lambda_n^2)^n}{(q^2 - \Lambda_n^2)^n}, \quad (2.4)$$

where  $n = 1, 2$ ,  $\mu = m_\pi$ , and  $\Lambda_n$  are free parameters. For realistic values of  $\Lambda^2$  ( $\Lambda^2 = 0.71\text{--}1.15 \text{ GeV}^2$ ) and a realistic (Paris) wave function, the theoretical estimates [7] are usually a factor 2–4 smaller than the experimental results [2,3]. According to the evaluations of ref. [7],  $\pi$ -meson exchange gives the largest contribution, dominant over the  $\rho$ -exchange.

A branching ratio three times larger than the experimental values [2,3] was predicted in ref. [5]. That result comes from a big contribution of  $\rho$ -exchange, presumably due [8] to the treatment of the diagram of fig. 1.

A contribution from a *direct one-meson annihilation* could be taken into account by allowing a nucleon of deuteron to be off mass-shell. The corresponding diagram is shown in fig. 2a: the invariant Mandelstam variable  $t$  is negative, and very large near the threshold (at rest):

$$t \approx -1.5 \text{ GeV}^2, \quad (2.5)$$

therefore the “neutron” is highly virtual, very far from the mass-shell  $t = m_N^2$ .

A reliable estimate of this contribution has never been performed. Some theoretical efforts are in progress [9].

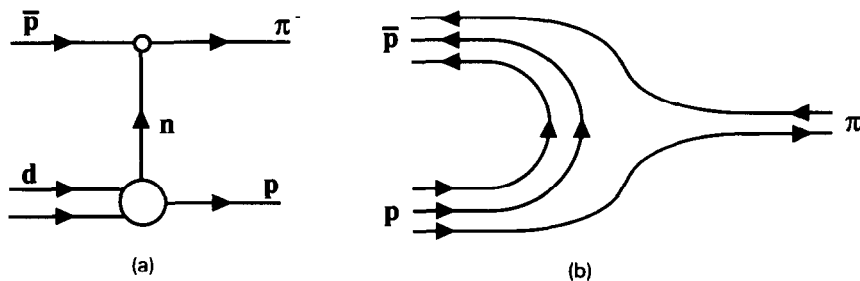


Fig. 2. Direct one-meson annihilation: (a) virtual nucleon exchange in the  $t$ -channel; (b) quark diagram for one-pion annihilation.

The interest in disentangling direct one-meson annihilations lies in the fact [9] that they can provide an important test of the microscopic models of antinucleon–nucleon annihilation at the quark level, since the process  $\bar{N}N \rightarrow \pi$  requires the simultaneous annihilation of at least two antiquark–quark pairs (see fig. 2b).

A first conclusion that can be drawn is that, within the framework of two-step processes, all mechanisms describing the simplest Pontecorvo reaction correspond to situations where either the two nucleons of deuteron are very close to each other or one of them is highly virtual. This is the case in which non-nucleonic degrees of freedom play an important role.

In this context, an admixture of multi-quark-states in the deuteron wave function was introduced in ref. [6]. It was indeed possible to increase the contribution of the triangle diagram of fig. 1 using a hybrid deuteron wave function containing an admixture of a 6-quark bag. For a 0.3% fraction of the 6-quark bag component, which is consistent with estimates from other sources, an agreement with the experimental results was obtained. It must be also stressed that, up to now, all calculations of the two-step sub-processes have been performed without taking into account absorptive corrections (initial-state interactions). These should lead to additional reduction of amplitudes, which would imply higher admixture of the 6-quark bag component in order to restore the agreement with experiment.

## 2.2. Regge-pole approach

The analysis of binary hadronic processes at high energies shows that, in order to take into account not only the nearest pole in the  $t$ -channel (the nucleon pole), but also contributions of other singularities, it is necessary to make a reggeization of the corresponding exchange. In other terms, when in a hadronic process the exchanged particle is far off mass-shell, as for the diagrams of Pontecorvo reactions of figs. 1 and 2a, the whole set of states on the corresponding Regge trajectory must be taken into account and reggeization should be applied. Strictly speaking, this prescription is valid for high energies, but, due to duality, it usually

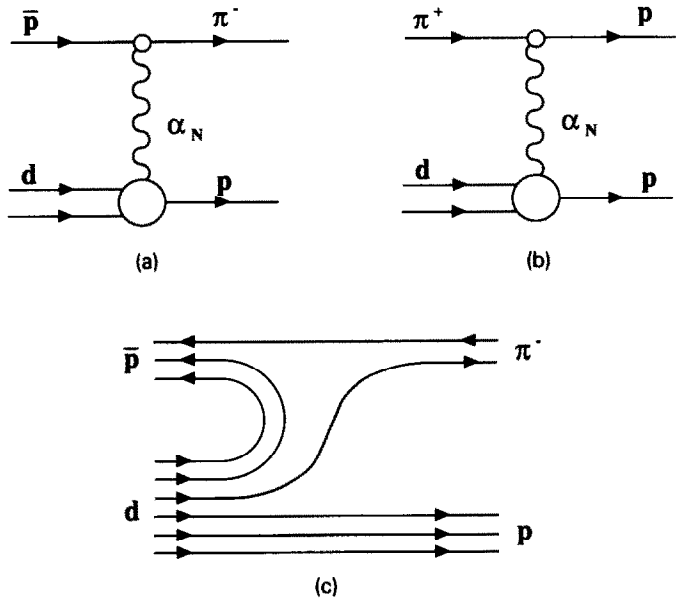


Fig. 3. Regge-pole approach to Pontecorvo reactions. Baryon Regge-pole-exchange diagram for: (a) direct reaction  $\bar{p} d \rightarrow \pi^- p$  and (b) crossed reaction  $\pi^+ d \rightarrow p p$ ; (c) planar quark diagram for the reaction  $\bar{p} d \rightarrow \pi^- p$ .

works, on average, in the medium and low-energy region. Since the physical region of the simplest Pontecorvo reaction starts at  $s^2 \geq 9m_N^2$ , this approach has been applied and considered approximately valid in ref. [10] (also in consideration of the fact that there are no narrow baryonic resonances in this region).

In ref. [10], the reaction  $\bar{p} + d \rightarrow \pi^- + p$  is described by the diagram of fig. 3a, in which the exchange of baryonic Regge poles in the  $t$ -channel has been considered. From the point of view of the  $1/N$  expansion of quantum chromo dynamics, the diagram of fig. 3a corresponds to a planar diagram with annihilation of diquarks of the antiproton and of the deuteron, as shown in fig. 3c.

The diagram with reggeized nucleon-exchange includes, at high energies, the contributions of both the triangle diagram of the conventional two-step process (fig. 1) and of the nucleon-exchange diagram in the direct one-meson annihilation of fig. 2a. The triangle diagram of fig. 1 is a particular case for the deuteron–reggeon–nucleon lower vertex of the diagram of fig. 3a.

In order to determine this vertex, the line-reversed reaction

$$\pi^+ + d \rightarrow p + p \tag{2.6}$$

or its time-reverse

$$p + p \rightarrow \pi^+ + d \tag{2.7}$$

has been considered. The corresponding diagram, which is obtained by that of the direct reaction in fig. 3a by interchanging, in the upper line, ingoing and outgoing particles, and particles with antiparticles, according to crossing symmetry, is reported in fig. 3b.

Connection between cross sections of direct and crossed reactions are due to crossing symmetry and to asymptotic relations for  $s \rightarrow \infty$ . At not too high energies, however, the physical regions of the variable  $t$  for the two reactions are different. This leads to a substantial difference between the total cross sections at intermediate energies. The model based on reggeon diagrams, by fitting [10] the  $p + p \rightarrow \pi^+ + d$  total and differential cross sections [11–13], is able to reproduce [10] the existing data of the Pontecorvo reaction [2,3], together with those of its time-reverse reaction  $\pi^- + p \rightarrow \bar{p} + d$  [14–16].

It is worth to observe [10] that in the model an effective trajectory of the nucleon Regge pole,  $\alpha_N(t)$ , is characterized by the condition

$$\alpha_N(t) < -0.5 \quad \text{for } t < 0, \quad (2.8)$$

which means that the state which is exchanged in the  $t$ -channel differs strongly (it has a different “spin”) from an “elementary” nucleon, which has  $\alpha_N = \frac{1}{2}$ . This fact can be interpreted as due to non-nucleonic degrees of freedom in the Pontecorvo reaction  $\bar{p} + d \rightarrow \pi^- + p$  at all energies, and in the crossed reactions  $p + p \rightarrow \pi^+ + d$ ,  $\pi^+ + d \rightarrow p + p$  at medium and high energies.

### 2.3. Statistical model

The basic premise of the statistical-model approach to antinucleon annihilation [17] is that annihilation is a rather complicated process, which involves a strong rearrangement of the parton structure. It is very much alike to the compound nucleus formation for the nucleons. This analogy suggests, quite naturally, the application of statistical methods to the decay of systems (“fireballs”) characterized by baryonic number  $b = 0$ , in case of single-nucleon (ordinary) annihilations, or baryonic number  $b > 0$ , for (unusual) annihilations of two, or more, nucleons. The Pontecorvo reactions, which require the cooperation of (at least) two nucleons at the same time, can be considered  $b \geq 1$  annihilations, although, as we have shown, they can be also pictured as due to the re-absorption of off-shell mesons. However, it is not sure that the two approaches exclude each other and that they are not merely two descriptions of the same physical reality using different words and different degrees of complexity. We shall come back to this point.

The existence of a  $b = 1$  annihilation means that, beyond the ordinary mechanism of annihilation on a single nucleon, in a fraction of cases the primary stage may indeed involve two nucleons. The scenario could be the following [17]: the

collision of an incoming antiproton with a nucleon leads to the formation of a hadronic fireball with  $b = 0$ , a finite lifetime  $\tau_f$ , and a non-vanishing velocity  $\beta_f$ . This fireball may collide with another nucleon inside the nucleus and *coalesce* with it forming a  $b = 1$  fireball, which eventually decays into a number of hadrons inside the nucleus.

Both  $b = 0$  and  $b = 1$  fireballs decay statistically into stable hadrons according to a microcanonical approach, in the sense that energy and baryon numbers are exactly conserved. As usual in statistical models, the invariant transition matrix does not depend very much upon the characteristics of the final states, i.e. the decay is dominated by the available phase space.

Application of the statistical model to  $b = 0$  annihilations looks successful in reproducing branching ratios for many final states, pion multiplicity distributions, pion momentum spectra, etc. This was obtained with the help of only three parameters (for annihilation at rest).

The observation of a Pontecorvo reaction [2,3], represents [17] a demonstration of the existence of  $b = 1$  annihilations. But to apply the statistical model to  $b = 1$  annihilations is not straightforward. First, the model needs, in such a case, a fundamental parameter: the formation probability of the fireball. This was indeed estimated by using a simple geometrical model [17,18], with reasonable guesses on the main physical quantities, but without (elaborate) cascade calculation. It can also be deduced from experimental information. In the case of the  $\bar{p} + d \rightarrow \pi^- + p$  reaction, the model predicts [17] a branching ratio for the  $b = 1$  fireball decay of  $3.4 \times 10^{-4}$ . The formation frequency was attributed recalling an experimental study of the reaction  $\bar{p} d \rightarrow \Lambda K \pi$ 's [2], where a large fraction of events (about 10%) could not be described by  $K^+$  rescattering, but had to be considered genuine  $b = 1$  annihilations ("three-body annihilations", in the old terminology). Therefore, under the assumption that the probability for  $b = 1$  fireball formation in deuterium was  $\approx 10\%$ , a rate of  $\sim 3 \times 10^{-5}$  was obtained.

The second questionable point of the statistical approach is represented by its application to unusual annihilations. Indeed, the statistical model can give reasonable predictions for the main channels of annihilation, but it cannot, in principle, work as well for very rare channels, like the Pontecorvo reactions, whose probabilities are of order of  $10^{-5}$  or less. In such cases, dynamics, which is ignored in such a model, should be essential. Indeed dynamic selection rules are important for two-body final states in  $\bar{N}N$  annihilation.

The interesting question is to understand whether the statistical approach bears some relationship with the current dynamical models which adopt the quark structure. In the simplest Pontecorvo reaction, if the two nucleons are close enough, it is reasonable to admit that an antiquark of the incoming antinucleon annihilates with a quark of one nucleon, while the two other antiquarks annihilate with two quarks of the other nucleon. This corresponds to an annihilation on two nucleons. In this sense, the  $b = 1$  annihilation considered by the statistical model

Table 1  
Theoretical predictions for the branching ratio of the reaction  $\bar{p} + d \rightarrow \pi^- + p$

Two-step process with meson exchange	Regge-pole approach	Statistical model
Kondratyuk and Sapozhnikov [7]: $2-6 \times 10^{-6}$ ( $A^2 = 0.71-1.15 \text{ GeV}^2$ )	Kaidalov [10]: $1.4 \times 10^{-5}$	Cugnon and Vandermeulen [17]: $\approx 3 \times 10^{-5}$
Hernandez and Oset [5]: $3.8 \times 10^{-5}$		
Kondratyuk and Guaraldo [6]: $\approx 1.5 \times 10^{-5}$ (0.3% admixture of 6-quark bag)		

requires non-nucleonic degrees of freedom. Along this line, both approaches: the statistical model applied to the decay of a fireball with  $b > 0$ , and the sub-process involving the absorption of hadrons off mass-shell, showing evidence for non-nucleonic degrees of freedom in nuclei, can be considered different descriptions of the same features of the physical process.

In table 1 the numerical evaluations obtained by the different models for the branching ratio of the Pontecorvo reaction  $\bar{p} + d \rightarrow \pi^- + p$ , are reported.

### 3. Experimental

The measurement was performed at the CERN low-energy antiproton ring (LEAR), with the OBELIX spectrometer, located at the M2 branch. A description of the experimental apparatus can be found in ref. [19]. Fig. 4 gives a sketch of the OBELIX facility. It consists of four sub-detectors arranged inside and around the open axial field magnet (OAFM).

The data were collected during the first (September 1990) runs of OBELIX, mostly devoted to debugging and calibrations. At that moment, two of the four sub-detectors, the jet drift chambers (JDC) and the time-of-flight (TOF) system, were operational, and a third, the spiral projection chamber (SPC) vertex detector, was at the very early stage of debugging. Furthermore, the data-acquisition rate was limited to less than 10 events/s. These circumstances forced us to use the spectrometer for the study of the  $\bar{p}d \rightarrow \pi^- p$  reaction in a quite unusual and, at first sight, not very efficient way. Monte Carlo simulations showed that, with the features of the spectrometer then standing, the number of true events that could be written on tape was maximized by using only a reduced part of the available solid angle, but requiring on the active parts quite tight trigger conditions that reduced the number of background events. In other words, OBELIX was used as a

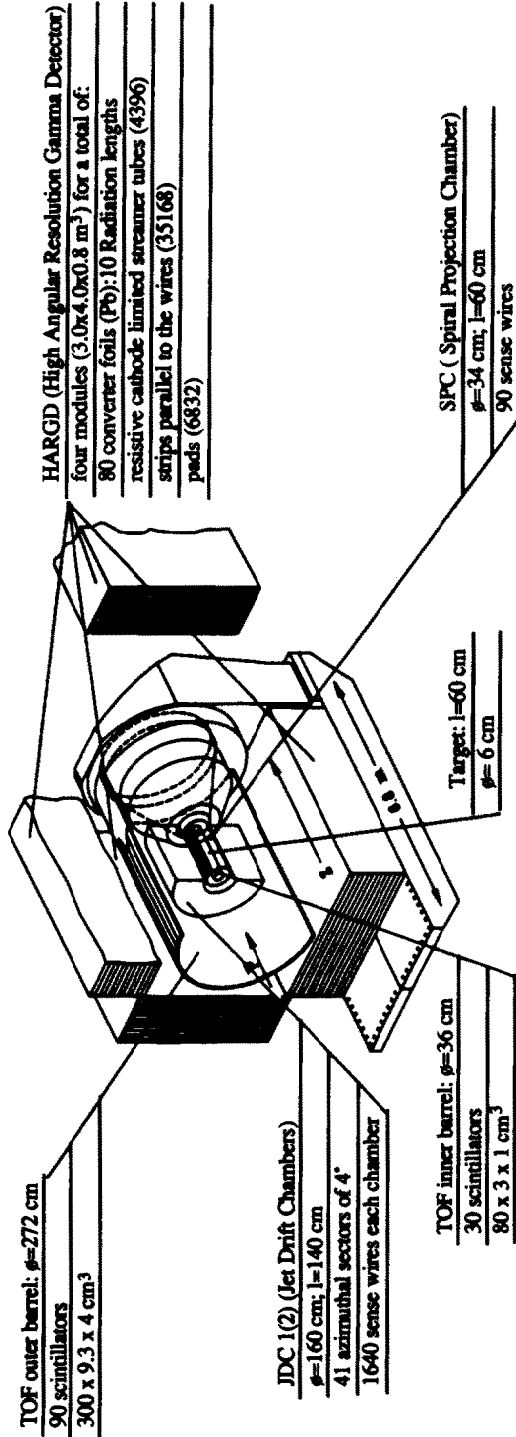


Fig. 4. Layout of the OBELIX spectrometer.

two-arm magnetic spectrometer, subtending a small ( $\approx 100$  msr) solid angle, as usually done for the study of two-body reactions at low rates. The usefulness of such a strategy was demonstrated by the fact that a reasonable number of events was collected in a rather reduced time ( $\approx 15$  hours).

Moreover, just due to the debugging stage of the experiment, a part of the data was collected with a large gaseous target and a part with a smaller one, which was solidal with the SPC and, even if less suitable in providing clean events, was helpful in understanding the performances of such a detector.

### 3.1. Data taking and trigger configurations

The antiprotons of 105.5 MeV/c momentum ( $\Delta p/p \leq 10^{-3}$ ) delivered by LEAR, after passing a 100  $\mu\text{m}$  Be window, crossed a 80  $\mu\text{m}$  beam scintillator counter, which gave the start to event timing and trigger logic, and entered the target through a 78  $\mu\text{m}$  mylar window. The momentum at the target entrance was  $\approx 60$  MeV/c, with a dispersion of  $\approx 1\%$ . Due to range straggling and multiple scattering, the annihilation vertex distribution had a spread, around the center of the target, with  $\sigma_z \approx 5$  cm along the beam axis and  $\sigma_x \approx \sigma_y \approx 2$  cm in the transverse plane. The beam spread in the transverse plane, combined with the target dimensions and the fluctuations in beam alignment, allowed a fraction of annihilations to occur on the target mylar walls when the smaller target was used. However, as described in sect. 3.5, one could separate the annihilations on target walls from those in the gas by measuring the position of annihilation vertices and by using the time-of-flight information. Annihilations in flight were evaluated to amount to some parts per thousand of the total annihilation rate. Annihilations on the target entrance window were evaluated to be less than 1% and could in any case be recognized.

*Trigger configurations.* The trigger was designed to select the topology of an event characterized by two correlated back-to-back long tracks belonging to high-momentum charged particles. The background contaminating the signal was constituted mainly of reactions with a spectator neutron:  $\bar{p}d \rightarrow \pi^+\pi^-n_s$  and  $\bar{p}d \rightarrow K^+K^-n_s$ . The data were collected under two different trigger configurations:

*HARD trigger.* This required the coincidence of the beam-counter signal with a highly selective back-to-back correlation in the TOF barrels. Specifically, it was requested: only two hits in the inner barrel, on two opposite slabs chosen among three adjacent ones; only two hits in the outer barrel, on two opposite slabs chosen among two adjacent ones ( $\pm 8^\circ$  in azimuthal angle). The external slabs were fixed in the measurement, thus selecting the back-to-back trigger configuration.

*SOFT trigger.* This was characterized by a looser request on the outer barrel: two hits on two opposite slabs chosen among three adjacent ones ( $\pm 12^\circ$  in azimuthal angle).

Moreover, a significant difference between the two data-taking configurations was represented by the experimental set-up adopted in the two cases. In data taking with the HARD trigger, a large deuterium gas target of 30 cm diameter, 75 cm length was used. In the SOFT trigger, the small target solidal with SPC (6 cm diameter, 60 cm length, 12  $\mu\text{m}$  thick mylar walls) was used. Overall, about  $7 \times 10^4$  events using the HARD trigger and about  $6 \times 10^4$  events using the SOFT trigger were collected in the same running period. Moreover, a sample of about  $10^4$  minimum bias events, triggered on the incoming antiproton, was also collected.

### 3.2. Trigger efficiency

The efficiency of the inner and outer TOF slabs participating to the trigger was evaluated from the sample of minimum bias events. On the external barrel, the two trigger configurations involved two opposite groups of two slabs and two opposite groups of three slabs, respectively. Correspondingly, due to the geometry of the tracks accepted by the trigger, two opposite groups of two slabs turned out to be fired on the inner barrel.

As far as the efficiency of the slabs of the inner barrel participating to the trigger is concerned, the average number of hits over the interested slabs was referred to the average efficiency of the inner barrel, as measured from minimum bias data for events with various multiplicities. In the HARD trigger, the total efficiency turned out to be  $\approx 93\%$ . In the SOFT trigger, the total efficiency was  $\approx 89\%$ .

As far as the external barrel is concerned, the slabs inserted in the trigger registered comparable numbers of hits, consistent with the counting efficiency of every other slab of the external barrel. A total efficiency of  $\approx 98\%$  was deduced.

From the above values, the global efficiency,  $\epsilon_t$ , of the TOF slabs participating to the trigger turned out to be  $\epsilon_t \approx 91\%$  for the HARD configuration and  $\epsilon_t \approx 87\%$  for the SOFT configuration.

### 3.3. Off-line calibrations

An estimate of the relative displacement of the two JDC chambers was obtained by using back-to-back  $\bar{p}p \rightarrow \pi^+\pi^-$  events, collected in the same data taking. The difference between the impact parameters of negative and positive prongs, used as alignment parameter in the  $R\phi$  plane, gave a relative displacement in the direction along which the chambers could be moved,  $\Delta_x = 3.5 \pm 1$  mm. Along the  $y$  and  $z$  directions, the mechanical alignment was known within 0.1 mm.

The same back-to-back  $\pi^+\pi^-$  data sample was used for a cross-check of the calibration of the TOF system. The accuracy in time alignment of the various slabs turned out to be better than 300 ps, and the time-of-flight resolution  $\Delta_{\text{TOF}}(\text{FWHM}) = 1.2$  ns.

### 3.4. Detector response and physics simulation

The OBELIX Monte Carlo simulation program is based on the GEANT package [20]. As far as the detector response is concerned, efficiency maps of the JDC wires and of the TOF slabs were extracted from minimum bias data and introduced in the simulation. The number of inactive sense wires amounted to  $\approx 5\%$  of the total. The drift time response of the JDC was calculated from a look-up table obtained by the GARFIELD program [21]. Electron diffusion, Lorentz angle and drift velocity dependence on electric and magnetic field were taken into account, as well as the drift path dependence on the track angle in the drift cell. Major systematic effects, like electrostatic sagitta, direct-shadow asymmetry in the charge collection, signal-propagation time in the sense wire and particle-propagation time in the chambers, which were taken into account in the reconstruction program, were introduced in the simulation. The JDC momentum resolution was reproduced by properly smearing the drift time and the charge collected by the wires. The TOF time resolution was reproduced by a gaussian resolution function whose parameters were deduced from the real data sample after the time-calibration correction.

The geometrical acceptance of the apparatus for the Pontecorvo reaction,  $\epsilon_g$ , was calculated by taking into account the experimental beam-spot distribution, as deduced from minimum bias data. It turned out to be  $\epsilon_g = 0.8\%$ , corresponding to a solid angle  $\Delta\Omega_H \approx 100$  msr, for the HARD trigger and  $\epsilon_g = 1.19\%$ , corresponding to a solid angle  $\Delta\Omega_S \approx 150$  msr, for the SOFT trigger.

As far as the simulation of the annihilation mechanism is concerned, the  $\bar{p}d$  annihilation reaction was allowed to proceed either on a pair of nucleons or on a single nucleon, with a nucleon momentum distribution given by a Hultén wave function.

Once the annihilation channel was chosen randomly on the phase space, pion and kaon branching ratios, as deduced from statistical models, were used. The momentum of the outgoing mesons was generated according to the Lorentz-invariant phase-space model using the CERN phase-space routine GENBOD, derived from the program FOWL [22]. In this simulation mode, mesons were modelled globally, without treatment of mesonic resonances.

### 3.5. Total number of annihilations

The total number of annihilations in the target was measured using the TOF inner barrel of scintillator counters. Each slab of the inner barrel was read out in a timing coincidence triggered by the beam counter signal and sensitive only to particles produced by annihilations nearly in the central region of the target (this was selected by a ns gate centered on the signal peak: see fig. 5d) giving at least one hit on the TOF inner barrel. This coincidence gave the GORFI signal (GORFI: Gated OR toF Inner). The gated coincidence satisfying the trigger

requirement, the TRIGGER signal, started the event acquisition. All the counter scalers were inhibited during the read-out of an event. Whenever two incoming antiprotons hit the beam counter in a time interval shorter than the formation time of the signal from the slowest detector, a signal from the pile-up rejection circuit stopped the event acquisition and the EVENT scaler was not implemented. The ratio EVENT/TRIGGER is an estimate of the percentage of the not piled-up GORFI signals.

The accumulated rates of signals GORFI, TRIGGER and EVENT were used to evaluate the integrated number of annihilations in deuterium:

$$N_{\text{ann}} = N(\bar{p} d \rightarrow \text{all}) = N_{\text{ann}}^{\text{d}}(1 + \epsilon_n)(1 - \epsilon_m), \quad (3.1)$$

where

$N_{\text{ann}}^{\text{d}}$  = GORFI EVENT/TRIGGER is the number of detected annihilations,

$\epsilon_n$  is the loss factor for undetected events,

$\epsilon_m$  is the contamination factor due to the target mylar walls.

*Evaluation of the loss factor  $\epsilon_n$ .* The OBELIX Monte Carlo program was used to evaluate the global amount of losses,  $\epsilon_n$ , of events undetected by the GORFI coincidence, i.e. annihilations in neutral final states without converted photons, and events with undetected prongs or due to the geometrical acceptance of the TOF inner barrel or for the inefficiency of the scintillator slabs: in other words, “zero-prong” events.

The  $\bar{p} d$  annihilations were simulated as a 55%/45% mixing of  $\bar{p}p$  and  $\bar{p}n$  annihilations, taking in such a way into account the experimental ratio of the annihilation cross sections on protons and on neutrons [23,24]. The experimental multiplicities obtained from  $\bar{p}LH$  and  $\bar{p}LD$  data in literature [25] were used, together with the vertex distribution as deduced from the minimum bias data collected in the measurement. Decay of neutral particles and photon conversion were taken into account. Moreover, the tracking in the apparatus of the spectator proton was performed. The average inefficiency of the TOF inner barrel (3%) was not included at the simulation level, but it was taken into account in treating those events which gave only one hit on the inner barrel. The results are summarized in table 2.

From table 2, the loss factor  $\epsilon_n$  for undetected “zero-prong” events turned out to be 1.8%.

*Evaluation of the contamination factor  $\epsilon_m$ .* Annihilations on the mylar walls of the target could contribute both to the event sample and to the total number of annihilations. As far as the HARD trigger data sample is concerned, the extended target size kept the contamination from the target walls negligible. On the contrary, in the SOFT trigger configuration the beam spot tails could intercept the target walls.

The background from the mylar walls was evaluated using the minimum bias data sample. The events were selected with the requirement of a prong multiplicity

Table 2  
Loss factor for “zero-prong” events

Monte Carlo minimum bias events	$\geq 1$ hit events (%)	loss for slabs inefficiency (%)	Global acceptance (%)
$\bar{p}pn_s$	97.2	0.2	97
$\bar{p}np_s$	99.9	0.6	99.3
$\bar{p}d$			98.2

greater than 2 and a reconstructed vertex. Annihilations on complex nuclei are characterized by a time of the antiprotonic atom cascade the shorter the heavier the nucleus [26]. In fig. 5a the distribution of the average annihilation times, defined as the time intervals between the antiproton signal at the beam counter and the average of the times measured by the slabs of the TOF inner barrel, is shown. The region below about 30 ns can be interpreted as dominated by annihilations on the target walls (“background region”); the region above about 30 ns contains mostly annihilations on deuterium (“signal region”). The distribution of the average annihilation times versus the radial distance of the vertex from the target axis, shown in fig. 5b, confirms that the events of the “background region” were indeed generated on the target walls (3 cm from the target axis). The fraction of background events was evaluated by examining the scatter plot of the annihilation time versus the  $z$  coordinate of the vertex (fig. 5c). The “signal region” and the “background region” could be separated by a cut along the straight line  $T_{\text{ann}} = AZ_{\text{vert}} + B$ , where  $A$  and  $B$  are constants. The background fraction turned out to be  $\approx 32\%$ . Finally, in the 10 ns gate of the GORFI coincidence the target wall contamination fraction,  $\epsilon_m$ , turned out to be  $(4 \pm 1)\%$ , the error being due to the uncertainty on the parameters  $A$  and  $B$  (see fig. 5d).

## 4. Data analysis

### 4.1. Event selection: the quality cut

Only events with two reconstructed tracks of opposite sign were accepted. A filter on the track quality was applied. In the region of 1 GeV/ $c$  the multiple-scattering contribution to the momentum resolution was negligible in comparison with the intrinsic resolution of the drift chamber. The intrinsic resolution depends on the transverse length  $l_t$  in the  $(x, y)$  plane and on the number  $N$  of points of the track as  $(L_t^2 \sqrt{N})^{-1}$  [27]. The parameter used to select the best quality tracks, i.e. tracks with the best resolution, was therefore the track length  $L_t$ . The best resolution at the  $\pi^+ \pi^-$  momentum peak was obtained with  $L_t \geq 50$  cm, corresponding to tracks traversing all the three crowns of the drift chamber. If all tracks were emitted by a point-like source at the center of the detector, tracks with a dip angle  $|\lambda| < 41^\circ$  [ $\lambda$  is the angle of the track with the  $(x, y)$  plane] should cross all

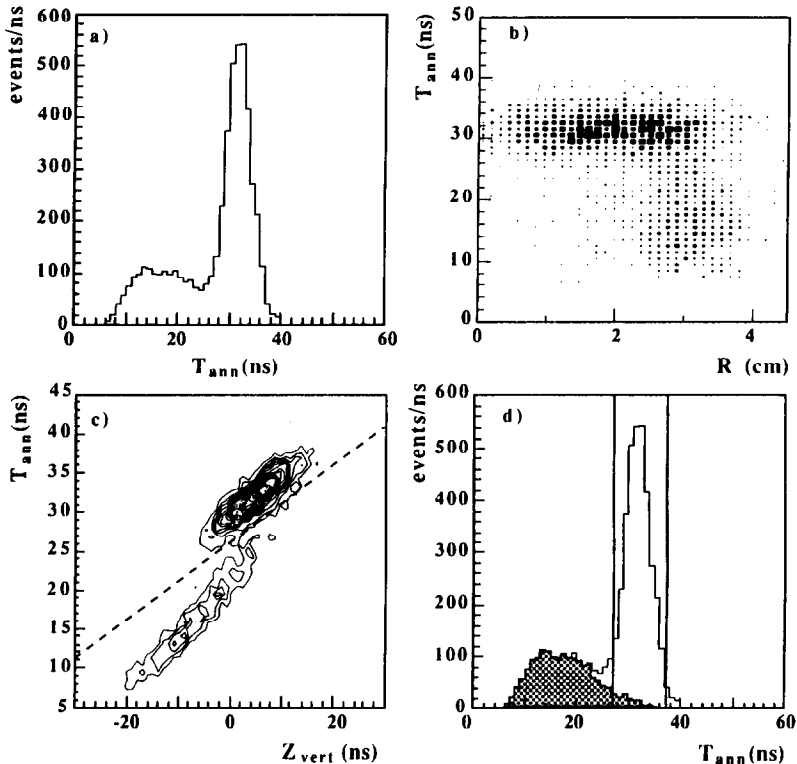


Fig. 5. Evaluation of the target mylar walls contamination: (a) distribution of the average annihilation times; (b) distribution of the average annihilation times versus the radial distance of the annihilation vertex from the beam axis; (c) scatter plot of the average annihilation times versus the  $z$  coordinate of the vertex, with separation of the “signal region” from the “background region”; (d) distribution of the average annihilation times: the shaded area is the background region, of which a fraction, equal to  $(4 \pm 1)\%$ , falls within the 10 ns gate centered on the signal.

the layers of the third crown of the chamber (in such a case  $L_t \geq 60$  cm). Thus, in order to select long tracks, a fiducial volume, defined by the requirement to have both tracks of an event dipped less than  $41^\circ$ , was introduced. Eventually, an event was accepted as a good quality event if the two tracks lying in the fiducial volume had transverse length, measured from the first to the last point of the fit, greater than 50 cm.

*Fiducial volume selection.* The efficiency of the event selection performed by introducing the fiducial volume was numerically evaluated comparing real and Monte Carlo acceptances for the reaction  $\bar{p}d \rightarrow \pi^+\pi^-n_s$ . The  $\pi^+\pi^-n_s$  events in the real data sample had been previously selected by a collinearity cut,  $\theta_{12} > 175^\circ$ , and by a cut on momenta:  $p_1, p_2 \geq 850$  MeV/c, in order to reduce the contamination from  $K^+K^-n_s$  events. From table 3, a good consistency between simulated and real data can be seen. The Pontecorvo event acceptances were then deduced from the Monte Carlo data. The results are reported in table 3.

Table 3  
Fiducial volume selection

	Fiducial volume acceptance	
	HARD trigger	SOFT trigger
$\pi^+\pi^-\pi_s$ Monte Carlo data	98%	91%
$\pi^+\pi^-\pi_s$ real data	98%	92%
Pontecorvo ( $p\pi^-$ ) Monte Carlo data	90%	82%

From table 3, the fiducial volume acceptance,  $\epsilon_v$ , turned out to be  $\epsilon_v = 90\%$  for the HARD configuration and  $\epsilon_v = 82\%$  for the SOFT configuration.

*Efficiency of the quality cut.* Inefficiencies in patterns recognition and in track reconstruction could prevent some long tracks from being fitted up to the third crown; moreover, due to the beam spread along the  $z$ -axis, some tracks dipped less than  $41^\circ$ , but exiting from the chamber before reaching the third crown, could enter the geometrical acceptance of the fiducial volume. These two effects were taken into account in evaluating the efficiency of the quality cut. As far as the fiducial volume acceptance is concerned, the efficiency of the quality cut was deduced by comparing real and Monte Carlo data for the  $\pi^+\pi^-\pi_s$  events. The  $\pi^+\pi^-\pi_s$  events in the real data sample had been previously selected by the collinearity and momentum criteria. The results are summarized in table 4.

From table 4, the quality cut efficiency,  $\epsilon_q$ , turned out to be  $\epsilon_q = 76\%$  for the HARD configuration and  $\epsilon_q = 72\%$  for the SOFT configuration.

#### 4.2. Selection of the Pontecorvo events

The events were reconstructed by the OBELIX reconstruction program. The program was required to perform a vertex fit in the target region; if the fit failed, due to the high degree of collinearity of the tracks, the track parameters were

Table 4  
Efficiency of the quality cut for the HARD and (SOFT) trigger configurations

	$L_t > 50$ cm tracks in the fiducial volume (%)		Geometrical inefficiency (%)		Reconstruction inefficiency (%)		Global inefficiency (%)	
$\pi^+\pi^-\pi_s$ Monte Carlo data	96	(94)	4	(6)	–	4	(6)	
$\pi^+\pi^-\pi_s$ real data	81	(77)	4	(6)	16	(18)	19	(23)
Pontecorvo ( $p\pi^-$ ) Monte Carlo data	90	(88)	10	(12)	16	(18)	24	(28)

extrapolated up to the minimum approach point to the beam axis. The reconstruction efficiency,  $\epsilon_r$ , as deduced by scanning about 5000 events of each data sample, turned out to be  $\epsilon_r \approx 94\%$  for the HARD trigger and  $\epsilon_r \approx 89\%$  for the SOFT trigger.

The  $\beta$  versus momentum distribution, for positive and negative particles ( $\pi^\pm$ ,  $K^\pm$ ,  $p$ ), after applying the selections for correct sign assignment and high-quality tracks, is shown in fig. 6 (HARD trigger sample). Up to about 1 GeV/c like particles of opposite sign are about numerically equivalent, with a slight systematic presence in the positive ones of lower- $\beta$  particles (protons, which can not be ascribed to the target walls contamination, since the data refer to the HARD trigger sample). Above about 1 GeV/c, the channel of direct proton production through the Pontecorvo reaction is clearly opened and the  $\beta$  of the positive particles drops with respect to that of the negative ones ( $\pi^-$ ).

The momentum distribution for collinear events ( $\theta_{12} \geq 175^\circ$ ) shows the peaks of the background channels  $K^+K^-n_s$ , around 798 MeV/c, and  $\pi^+\pi^-n_s$ , around 928 MeV/c, together with a clear signal of the Pontecorvo reaction at the correct kinematical position of 1.25 GeV/c (fig. 7, HARD trigger sample).

A first filter was introduced to select events containing a proton through a  $3\sigma$  cut on the time of flight of positive particles. The kinematical fit procedure was then used to separate Pontecorvo events from background contamination.

The Pontecorvo hypothesis is based only on measured charged particles, therefore the fit has four kinematical constraints (4C-fit). The fit has one constraint

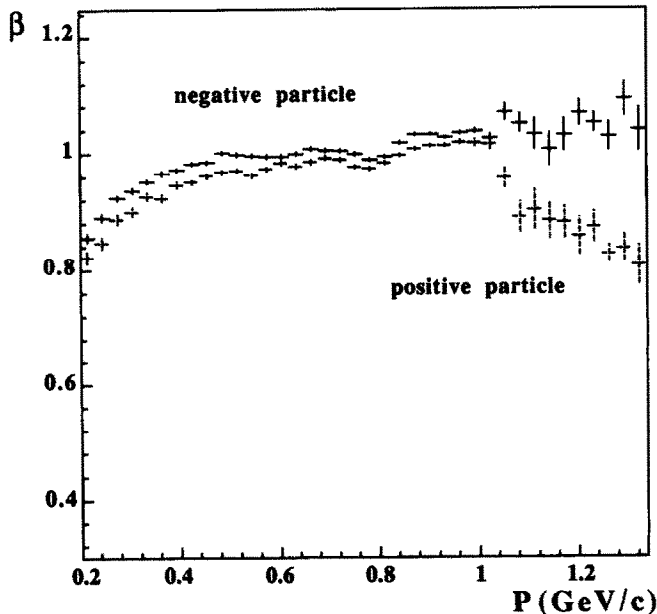


Fig. 6.  $\beta$  distribution versus momentum for positive and negative particles.

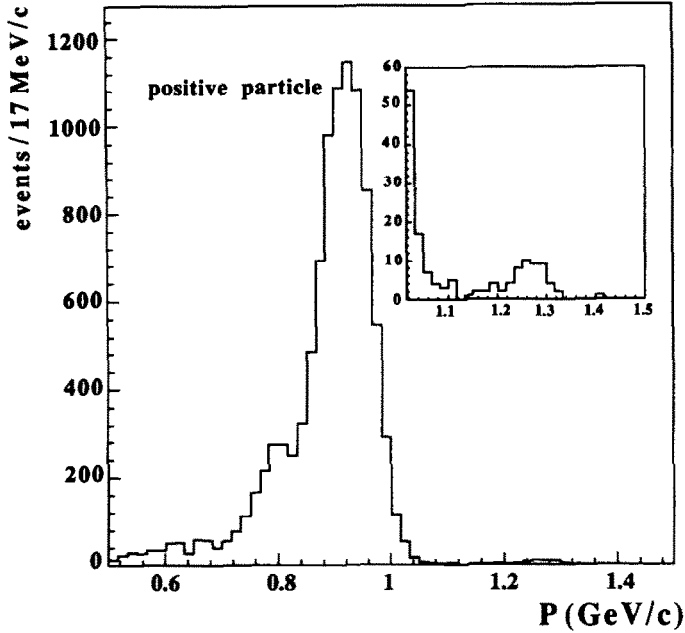


Fig. 7. Positive-particle momentum distribution for collinear events.

(1C-fit) if one neutral particle in the final state is unobserved, as occurs, for example, for the background reactions with the spectator neutron. The data sample was then submitted to the 1C-fit to the hypotheses  $\pi^+\pi^-n_s$  and  $K^+K^-n_s$ , in order to eliminate such contaminations. A cut at the confidence level of 1% (events with  $\chi^2 < 10$ ) was applied. After these selections, all positive particles with momentum  $> 1$  GeV/c were classified as protons.

Finally, the data sample was submitted to a 4C kinematical fit to the hypothesis  $p\pi^-$ . However, the accuracy in the measurement was not good enough to rely only on the result of this fit. Therefore, the possible contamination from channels containing one (or more)  $\pi^0$ 's was evaluated through a 1C kinematical fit to the  $p\pi^-\pi^0$  hypothesis. Fig. 8a shows the 4C  $\chi^2$  distribution of events, versus the 1C  $\chi^2$  distribution, for the HARD trigger data sample. On both distributions, a cut at a kinematical fit confidence level  $\epsilon_\chi = 4\%$ , corresponding to  $\chi^2(4C) = 10$  and to  $\chi^2(1C) = 4.4$  was applied (see fig. 8). Events with  $\chi^2(4C) < 10$  and with  $\chi^2(1C) > 4.4$  were accepted as Pontecorvo events. Events with  $\chi^2(4C) < 10$  and with  $\chi^2(1C) < 4.4$  were ambiguous events, compatible with both hypotheses. The number of accepted Pontecorvo events was 50. The ambiguous events were 5 (see fig. 8b). Four of them were eventually attributed to the Pontecorvo channel on the basis of the highest relative  $\chi^2$ -probability [28]. The fifth was a  $p\pi^-\pi^0$  event. Therefore, the final number of good events turned out to be 54.

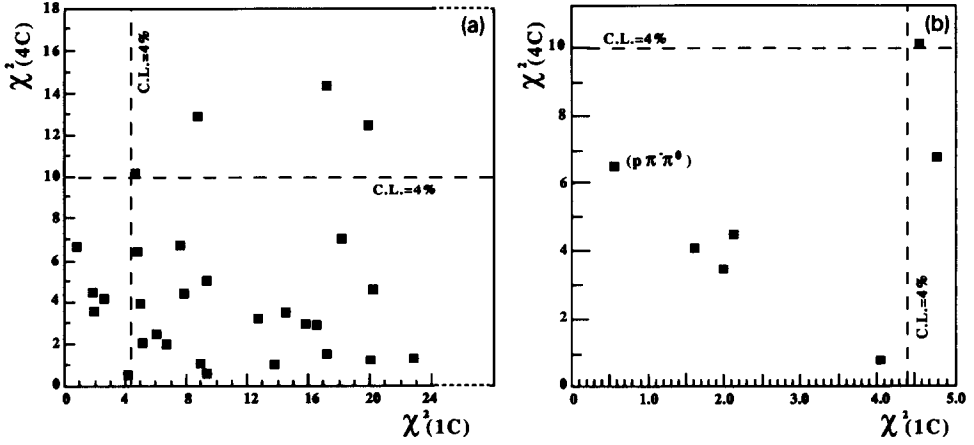


Fig. 8. (a) 4C  $\chi^2$  distribution of events for the  $p\pi^-$  hypothesis versus 1C  $\chi^2$  distribution for the  $p\pi^-\pi^0$  hypothesis. A cut at 4% confidence level, corresponding to  $\chi^2(4C)=10$  and  $\chi^2(1C)=4.4$  (dashed lines) is applied. Pontecorvo events are characterized by the two conditions  $\chi^2(4C) < 10$  and  $\chi^2(1C) > 4.4$ . Events in the region  $\chi^2(4C) < 10$  and  $\chi^2(1C) < 4.4$  are ambiguous events: they may be either good  $p\pi^-$  events or background  $p\pi^-\pi^0$  events. For all the events reported in the figure, the 1C fit could converge; (b) distribution of ambiguous events, to be assigned either to the Pontecorvo channel, or to the  $(p\pi^-\pi^0)$  channel.

A systematic error corresponding to 7 events, which could be assigned neither to the Pontecorvo channel nor to the background ones, should be considered. It comes from the calibration of the global system (see discussion at sect. 4.4).

As far as the SOFT trigger is concerned, by applying the same procedure, the number of Pontecorvo events was 20. The ambiguous events were 4. Three of them were eventually attributed to the Pontecorvo channel on the basis of the highest relative  $\chi^2$ -probability. Therefore the final number of good events turned out to be 23.

A systematic error corresponding to 3 not attributed events should be considered.

#### 4.3. Branching ratio of the Pontecorvo reaction

The absolute branching ratio for the reaction

$$\bar{p}d \rightarrow \pi^- p. \quad (4.1)$$

is defined as:

$$\text{BR}(\bar{p}d \rightarrow \pi^- p) = \frac{N(\bar{p}d \rightarrow \pi^- p)}{N(\bar{p}d \rightarrow \text{all})} = \frac{N_{\text{ev}}}{N_{\text{ann}}^d (1 + \epsilon_n)(1 - \epsilon_m)}, \quad (4.2)$$

Table 5  
Experimental parameters

	HARD trigger	SOFT trigger
Data sample	$7 \times 10^4$	$6 \times 10^4$
$N_{\text{ann}}^{\text{d}}$ – number of detected annihilations	$9.94 \times 10^8$	$3.66 \times 10^8$
$N_{\text{ev}}$ – number of Pontecorvo events	54	23
$\epsilon_n$ – “zero-prong” loss factor	0.018	0.018
$\epsilon_m$ – target wall contamination	–	0.04
$\epsilon_t$ – trigger efficiency	0.91	0.87
$\epsilon_g$ – geometrical trigger acceptance	0.008	0.0119
$\epsilon_v$ – fiducial volume acceptance	0.90	0.82
$\epsilon_q$ – quality cut efficiency	0.76	0.72
$\epsilon_r$ – reconstruction efficiency	0.94	0.89
$\epsilon_\chi$ – kin. fit confidence level	0.96	0.96

where:

$N(\bar{p}d \rightarrow \pi^- p)$  is the number of Pontecorvo events,  
 $N(\bar{p}d \rightarrow \text{all})$  is the total number of annihilations in deuterium,  
 $N_{\text{ev}}$  is the number of measured Pontecorvo events,  
 $N_{\text{ann}}^{\text{d}}$  is the number of detected annihilations,  
 $\epsilon$  is the product of the various efficiencies =  $\epsilon_t \epsilon_g \epsilon_v \epsilon_q \epsilon_r \epsilon_\chi$ .

Table 5 summarizes the relevant experimental parameters of the measurement for deducing the Pontecorvo branching ratio.

From (4.2) and table 5, one gets the values reported in table 6.

The weighted average of the branching ratios obtained with the HARD trigger and with the SOFT trigger, with its statistical error, is finally:

$$\text{BR}(\bar{p}d \rightarrow \pi^- p) = 1.20 \pm 0.14 \times 10^{-5}. \quad (4.3)$$

#### 4.4. Systematic effects

A certain number of systematic uncertainties have been studied. The most important of them are described below. They affected mainly the:

*trigger efficiency*: in evaluating the efficiency of the groups of slabs of the TOF barrels participating to the trigger, a systematic component of uncertainty, coming from the single-slab fluctuation around the average number of hits and from the normalization criteria adopted, could be estimated to be of the order of 5%.

Table 6  
Branching ratio of the Pontecorvo reaction ( $\bar{p}d \rightarrow \pi^- p$ ) for the two OBELIX data samples

	HARD trigger	SOFT trigger
BR ( $\bar{p}d \rightarrow \pi^- p$ )	$1.19 \pm 0.16 \times 10^{-5}$	$1.23 \pm 0.26 \times 10^{-5}$

*mylar contamination factor*: the evaluation of the fraction of background events coming from the target mylar walls could not take into account in a quantitative way the fluctuations of the beam position and the possible crossing of the target walls from the beam tails. By examining the periodically recorded displays of the beam profiles and the  $(x, y)$  coordinates of the vertex distribution, this systematic uncertainty on the  $\epsilon_m$  factor was evaluated to be of the order of 1%;

*reconstruction efficiency*: a systematic uncertainty on the reconstruction efficiency could be evaluated to be of the order of 1.5%;

*kinematical fit selectivity*: a systematic error coming from the calibration of the whole detector had to be considered. It came mainly from the characteristic uncertainty given by tracks belonging to a momentum region – the high-momentum one – not statistically rich enough to perform a precise evaluation of the momentum resolution. This reflected on the selectivity of the  $\chi^2(4C)$  fit to the Pontecorvo events. At the moment of the measurement, a full comprehension of the detector performances was still in progress. Considering the number of events which could not be assigned, this global systematic uncertainty was evaluated to be around 13% both for the HARD and for the SOFT trigger configuration.

The contamination from cosmic-ray events was excluded by checking that the slabs fired in each event had a time sequence proper of a two-prong event coming from the target.

Summing up all the above systematic effects, the absolute branching ratio of the Pontecorvo reaction must be corrected by a factor

$$f_{\text{sys}} = 1.00 \pm 0.19. \quad (4.4)$$

## 5. Concluding remarks and future perspectives

The OBELIX determination of the absolute branching ratio of the Pontecorvo reaction  $\bar{p}d \rightarrow \pi^- p$  has been performed in a dedicated measurement, with data taking characterized by a trigger specifically designed to select the topology of a Pontecorvo event.

Experimental parameters like trigger efficiency, detector calibrations, effective number of annihilations, etc., as well as event-selection criteria, data analysis procedures, were carefully evaluated within the established performances of a powerful spectrometer such as OBELIX.

Systematic effects have been the object of accurate research: a global systematic uncertainty on the the calibration of the whole spectrometer was found to be the dominant source.

On the front of statistics, the overall sample of Pontecorvo events measured by OBELIX (77 events) is more than fifteen times greater than the number of events collected by the only counters experiment performed up to now [3].

In conclusion, the OBELIX measurement is able to fix the branching ratio of the Pontecorvo reaction. Recalling the theoretical predictions (see table 1), the result is well reproduced by the two approaches which involve sub-nucleonic degrees of freedom of the target. Within statistical and systematical uncertainties of the measurement, and within the present theoretical descriptions, the obtained branching ratio appears to imply a valuable quark configuration in the ground state of the deuterium target. This could be defined an experimental indication of quark degrees of freedom in nuclear physics.

### 5.1. Theoretical developments

On the theoretical side, all models are incomplete, as we have already underlined. The two-step calculations suffer the intrinsic difficulty to deal with short-distance (high-momentum) wave functions and with the form factor behaviour of off-mass-shell mesons. A reliable parametrization of virtuality, based on realistic parameters, has presented difficulties [7]. Taking into account also the fact that no absorptive correction has been included, the model substantially underestimates data and needs additional improvements. A proper treatment of the off-shell behaviour of  $\bar{p}N$  amplitude should be considered in the analysis, as well as more experimental information, in order to extract reliable parameters for the meson–nucleon–nucleon form factor, is needed.

The inclusion in the target wave function of an admixture of non-nucleonic degrees of freedom, like a 6-quark bag [6], has proved to be a successful way to restore the agreement with experiment. However, the model has just the fraction of quark admixture as free parameter: if the fraction of 6-quark component is known from other sources, one can deduce the branching ratio of the Pontecorvo reaction. Another limit is, of course, that the model being based on two-step sub-processes, it needs the same improvements required in the treatment of triangle diagrams.

Extrapolation of Regge-pole approach to the medium and low-energy region turned out to be extraordinarily successful in fitting data of the crossed reaction  $\pi^+ d \rightarrow pp$  and in reproducing the Pontecorvo reaction and its time-reverse one, with excellent agreement with the OBELIX result. However, the deep reasons for this surprising success are not fully understood. Concerning the Pontecorvo reaction, the extrapolation at rest is based on few experimental data: it would be essential for the quality of the fit to measure the reaction in flight at various momenta.

As far as eventual developments of the statistical model are concerned, there is the open question of principle whether a rare channel, like a Pontecorvo one, can be the decay channel of a microcanonical ensemble. Moreover, as it is known, the model can not predict an experimental rate, unless one makes *ad hoc* hypotheses

on the formation frequency of the  $b > 0$  fireball or – and this can be the development – to properly solve the complex dynamical problem.

## 5.2. Experimental perspectives

On the experimental side, the field of Pontecorvo reactions is practically still to be explored, but measurements present increasing difficulty as soon as one explores beyond the “elementary” antiproton absorption on deuterium at rest.

Keeping the focus on a deuteron target, the Crystal Barrel experiment at LEAR is able to give the first measurement of neutral Pontecorvo reactions such as

$$\bar{p} d \rightarrow \pi^0 n \quad (5.1)$$

or with neutral mesons decaying into  $\gamma$ 's or  $\pi^0$ 's ( $\eta, \eta', \omega \dots$ )

Clear signals have already been observed [29] and the analysis is in progress.

On the front of charged particles, OBELIX will give the “ultimate” value for the  $\bar{p} d \rightarrow \pi^- p$  branching ratio, characterized by a systematic error reduced to some percent and by the statistical error of a sample of about a thousand good Pontecorvo events, taking advantage of the final tuning of the whole spectrometer and of specific calibration measurements.

The most relevant future program on deuterium appears to be the study of Pontecorvo reactions in flight.

We have already mentioned the importance of these measurements for the reliability of the Regge-pole approach. But other interesting physical effects might be put in evidence [8]. The predictions of differential cross section at different energies exist so far only in the model of ref. [10]. The ratio

$$R(\bar{p} d \rightarrow \pi^- p) = \frac{\sigma(\bar{p} d \rightarrow \pi^- p)}{\sigma_{\text{tot}}(\bar{p} d)} \quad (5.2)$$

decreases rapidly with antiproton momentum.

The angular distribution is predicted to be practically flat for momenta up to  $\approx 500$  MeV/c. This is a non-trivial consequence of the model, because at 500 MeV/c, for example, the invariant variable  $t$  changes by  $1.7$  GeV<sup>2</sup> when  $\cos \theta$  passes from  $-1$  to  $+1$ . Indeed, it is well-known that in the elementary annihilation sub-process  $\bar{p} p \rightarrow \pi^+ \pi^-$  the experimental pion angular distribution is very anisotropic, even at low momenta (200–300 MeV/c). Therefore, a measurement of angular distributions at different energies could allow one to check the reliability of the Regge-pole approach.

Moreover, from the isotropy of the angular distribution up to 500 MeV/c predicted by the model [10], it is possible to obtain limits on the contribution of higher partial waves and thus on the effective interaction radius for the process, which is predicted to be small [8]:  $R \lesssim 1$  fm, found in the elementary  $\bar{N}N$  annihilation. This puts in evidence an interesting property of Pontecorvo reaction, i.e. the fact that three incident antiquarks annihilate on three quarks in a very reduced volume.

But the main physical interest in studying the Pontecorvo reaction  $\bar{p}d \rightarrow \pi^- p$  in flight lies at higher energies [8], although well within the LEAR domain. The suggestion comes from an old, never repeated, measurement [15] of the time-reverse reaction  $\pi^- + p \rightarrow \bar{p} + d$  at  $P_\pi = 4, 5$  and  $6$  GeV/c, corresponding to antiproton momenta in the direct reaction  $P_{\bar{p}} = 0.51, 1.25$  and  $1.95$  GeV/c, respectively. At 4 GeV/c the experimental angular distribution is flat, while, for increasing momenta, there is an indication for a forward dip: it occurs for  $\sin \theta < 0.5$  in the c.m. system. The point is the following: theoretical models based on simple baryon-exchange and on reggeon-exchange predict, at high momenta, not a dip but a maximum.

If new measurements of the Pontecorvo reaction in the momentum range 0.5–1.95 GeV/c would confirm the above reported forward behaviour of the differential cross section of the time-reverse reaction, it might indicate a completely new mechanism of annihilation. A result which could deserve a dedicated investigation.

The measurement – for the first time – of Pontecorvo reactions different from the classical ones on deuterium would bring not only new information on multinucleon unusual annihilations, but also would give the possibility to perform more stringent tests of the theoretical models. In fact, while the predictions of different models for the absolute rates are subject to rather big uncertainties, ratios of cross section of different reactions are much less parameter-dependent and would permit one to discriminate among the models. In the case of the statistical model, for example, the ratio between two different channels would eliminate *ab origine* the uncertainty on the formation frequency of the decaying system, provided, of course, that the fireballs have the same baryonic number (the probabilities would be different). Still taking advantage of a deuterium target, the measurement of Pontecorvo reactions with strangeness in the final state

$$\bar{p} + d \rightarrow K^0 \Lambda, \quad (5.3)$$

$$\bar{p} + d \rightarrow K^+ \Sigma^-, \quad (5.4)$$

is important because the presence of a new flavour must involve quark dynamics in the annihilation mechanism and require specific approaches. For instance, the reactions (5.3) and (5.4) have exotic quantum numbers in the  $t$ -channel and a simple Regge-pole exchange is impossible.

Table 7

Theoretical model predictions for the ratio between different Pontecorvo reactions

	Two-step sub-processes [4]	Reggeon- exchange [10]	Statistical model [18]
$R(K^0\Lambda)$	0.01	0.06	0.22
$R(K^+\Sigma^-)$	$2.7 \times 10^{-4}$	$6.6 \times 10^{-3}$	0.64
$R(^3\text{He})$	$(0.8-1.4) \times 10^{-3}$ ref. [6]	$3 \times 10^{-3}$	$\approx 0.1$

If we consider the ratio of the cross section of a Pontecorvo reaction with strangeness with the prototype Pontecorvo reaction:

$$R(K^0\Lambda) = \frac{\text{BR}(\bar{p} d \rightarrow K^0\Lambda)}{\text{BR}(\bar{p} d \rightarrow \pi^- p)}, \quad (5.5)$$

$$R(K^+\Sigma^-) = \frac{\text{BR}(\bar{p} d \rightarrow K^+\Sigma^-)}{\text{BR}(\bar{p} d \rightarrow \pi^- p)}, \quad (5.6)$$

the predictions of the models can differ also by orders of magnitude, as is shown in table 7, and therefore the experimental results should more easily select among the models. A hard experimental task is, of course, the measurement of branching ratios which are orders of magnitude smaller than that of the prototype Pontecorvo reaction. However, BR's of the order of  $10^{-7}$  are within reach of the present capabilities of OBELIX. A dedicated effort on higher-level triggers could push these limits up to  $10^{-8}$ .

The use of a  $^3\text{He}$  target allows the measurement of the more exotic Pontecorvo reaction, the mesonless  $b = 2$  annihilation:

$$\bar{p} + ^3\text{He} \rightarrow p + n. \quad (5.7)$$

Here the annihilation process, in which the pion stage appears to have been skipped, is doubly unusual because two virtual mesons have to be absorbed. This can explain the very low branching ratio predicted by all models, with the exception of the statistical one, which reinforces the doubts on the reliability of this approach when dealing with very rare channels. In table 7, the ratio  $R(^3\text{He})$ :

$$R(^3\text{He}) = \frac{\text{BR}(\bar{p}^3\text{He} \rightarrow pn)}{\text{BR}(\bar{p} d \rightarrow \pi^- p)} \quad (5.8)$$

is reported.

A measurement of this ratio would allow a clear cut between the statistical model and the dynamical ones.

Finally, one could consider the class of Pontecorvo reactions with a meson resonance ( $\rho$ ,  $a_2$ ,  $AX, \dots$ ) in the final state. The predicted branching ratios are indeed comparable, or even greater [7], with respect to the value for the  $\pi^- p$  reaction. However, the difficulties linked to the unambiguous detection of broad resonances, decaying into two or more detectable particles, seem very severe.

We would like to thank the technical staff of the LEAR machine group for their support during the runs.

## References

- [1] B.M. Pontecorvo, *Sov. Phys. JETP* 3 (1956) 966
- [2] R. Bizzarri et al., *Lett. Nuovo Cim.* 2 (1969) 431
- [3] J. Riedlberger et al., *Phys. Rev.* C40 (1989) 2717
- [4] L.A. Kondratyuk and M.G. Sapozhnikov, *Phys. Lett.* B220 (1989) 333
- [5] E. Hernandez and E. Oset, *Nucl. Phys.* A494 (1989) 533
- [6] L.A. Kondratyuk and C. Guaraldo, *Phys. Lett.* B256 (1991) 6
- [7] L.A. Kondratyuk and M.G. Sapozhnikov, *Few-Body Systems, Suppl.* 5 (1992) 201
- [8] A.B. Kaidalov, Frascati national laboratory internal report (1992) unpublished
- [9] S. Mrówczyński, Soltan institute internal report (Warsaw, 1992) unpublished
- [10] A.B. Kaidalov, *Sov. J. Nucl. Phys.* 53 (1991) 872
- [11] J.V. Allaby et al., *Phys. Lett* B29 (1969) 198
- [12] U. Amaldi et al., *Lett. Nuovo Cimento* 4 (1972) 121
- [13] H.L. Anderson et al., *Phys. Rev.* D3 (1971) 1536; D9 (1974) 580
- [14] C. Baglin et al., *Nucl. Phys.* B37 (1972) 639
- [15] A.J. Pawlicki et al., *Phys. Rev. Lett.* 31 (1973) 665
- [16] C. Evangelista et al., *Nucl. Phys.* B131 (1977) 54
- [17] J. Cugnon and J. Vandermeulen, *Phys. Lett.* B146 (1984) 16
- [18] J. Cugnon and J. Vandermeulen, *Phys. Rev.* C39 (1989) 181
- [19] A. Adamo et al., *Sov. J. Nucl. Phys.* 55 (11) (1992) 1732
- [20] CERN Programme Library-W5013
- [21] CERN Programme Library-W5050
- [22] CERN Programme Library-W505
- [23] R. Bizzarri et al., *Nuovo Cim.* A53 (1968) 956
- [24] R. Armstrong et al., *Phys. Rev.* D36 (1987) 659
- [25] J. Cugnon and J. Vandermeulen, *Ann. de Phys.* 14 (1989) 49 and references therein
- [26] H. Poth, Proc. Workshop on antimatter physics at low energy, Fermilab, Batavia 1986, and CERN-EP/86-105 (1986)
- [27] R.L. Gluckstern, *Nucl. Instr. Meth.* 24 (1963) 381
- [28] A.G. Frodesen, O. Skjeggstad and H. Töfte, *Probability and statistics in particle physics* (Universitetsforlaget, Bergen 1979) p. 424
- [29] K. Peters, *Sov. J. Nucl. Phys* 55 (1992) 786